Available Online: 10 March 2026 DOI: 10.54254/2753-7102/2026.32147

Ecological recovery after the 2020 August Complex Megafire: remote sensing, community risk, and social implications

Tiger Yang

Acellus Academy, Newton, USA

tiger.ivyapp@outlook.com

Abstract. Wildfires are among the most destructive natural disturbances, with far-reaching impacts on ecosystems, carbon balance, and substantial socio-economic consequences including health risks, property losses, and community displacement. The 2020 August Complex wildfire in northern California burned over 1 million acres, releasing 27.7 million metric tons of CO_2, and causing significant ecological and structural damage. This study assesses post-fire vegetation recovery using Landsat 8 NDVI data from 2020 to 2025. After radiometric and geometric correction, Normalized Difference Vegetation Index (NDVI) was derived from red and near-infrared bands to quantify vegetation cover changes. Pre-fire imagery showed high vegetation density, which sharply declined in 2021. Gradual recovery was observed from 2022 onward, nearing pre-fire levels by 2024, though some areas lagged due to poor soil and erosion. Analytic Hierarchy Process (AHP) scores dropped from 6.59 (2020) to 2.66 (2021), then recovered to 6.22 by 2024. Entropy values similarly declined from 6.384 to 3.126 post-fire, rising to 6.238 by 2024, confirming ecosystem recovery supported by rainfall, yet highlighting spatially heterogeneous regrowth. This study provides new insights into the dynamics of post-fire recovery and delivers critical evidence to guide policy, planning, and restoration practices in regions increasingly threatened by megafires. These ecological patterns also shaped the pace of community recovery, influencing local risk exposure, watershed stability, and long-term resilience planning. By integrating ecological metrics with social implications, this study underscores the importance of science-based decision-making in protecting communities increasingly threatened by megafires.

Keywords: vegetation recovery, remote sensing, wildfire, ecosystem resilience

1. Introduction

Wildfires inflict immediate physical destruction and pose long-term threats through air quality degradation, significant health impacts, and substantial economic costs to communities. Smoke from large fires can travel thousands of miles, affecting regional air quality, while financial losses mount from firefighting expenses and property damage. Although wildfires have historically occurred across North America, fire deficits caused by long-term declines in burning over millennia have increased the risk of catastrophic blazes [1]. These events

exacerbate climate change through massive greenhouse gas emissions and release harmful particulate matter that jeopardizes respiratory health [2-4].

The August Complex fire of 2020—California's largest recorded wildfire—burned over 1 million acres in northern California, resulting in severe ecological disruption, significant carbon release, and the destruction of hundreds of structures. In light of recent wildfires, such as those in Los Angeles, post-fire monitoring tools are increasingly critical for evaluating recovery and guiding management strategies [5]. However, despite numerous assessments following the August Complex fire, a gap remains in using remote sensing indicators like the Normalized Difference Vegetation Index (NDVI) to analyze long-term vegetation recovery in this event.

This study employs NDVI to assess vegetation regeneration after the August Complex fire, aiming to provide insights into ecological recovery processes and support improved post-fire management practices.

2. Material and methods

2.1. Study area and data collection

This study was conducted near the coast range of Northern California, which is usually a damp place with mild winters and hot summers. To assess the damages done and how the environment changed, we used the satellite Landsat 8 Operational Land Imager. The images were taken from Geospatial Data Cloud for the period of 2020 to 2025.

The satellite images were used based on clear sky conditions, having minimal cloud coverage to ensure NDVI calculations to be accurate [6]. Pre-processing steps include radiometric and geometric corrections, which were applied to standardize the image before analysis.

2.2. NDVI calculation

NDVI was calculated through the use of red and near-infrared spectral bands in the following equation:

$$NDVI = \frac{NIR - Red}{NIR + Red} \tag{1}$$

Where NIR correlates with the reflectance of the near infrared-band (e.g., Band 5 for Landsat 8). R represents the reflectance in the red band (e.g., Band 4 for Landsat 8). The index ranges from -1 to +1, where values near +1 indicate dense, healthy vegetation, while 0 or negative corresponds to soil, water bodies, or built-up areas [7]. The spatial resolution of Band 4 in the near-infrared range (0.6 to 0.7 μm) is 30 meters. Band 5 also offers a spatial resolution of 30 meters in both the visible red range (0.6 to 0.7 μm) and near-infrared range (1.55 to 1.75 μm).

Band 4 in the near-infrared range (0.76 to 0.90 μm) has a spatial resolution of 30 meters. Band 5 in the visible red range (0.6 to 0.7 μm), and Band 5 in the near-infrared range (1.55 to 1.75 μm), also offers a spatial resolution of 30 meters.

2.3. Image processing and analysis

All satellite images are processed by ArcGIS Pro 3.4, a geographical information system that helps people create and manage geographic data.

2.4. Vegetation percentage calculation

Vegetation percentage can be estimated using NDVI with a linear scaling approach that relays NDVI values to the fractional vegetation cover. This method is based on the fact that NDVI can be normalized by the values between known reference values for bare soil and full vegetation cover, which allows the vegetation percentage to be calculated by the following formula [8, 9]:

$$\text{Vegetation Percentage} = \frac{NDVI_{pixel} - NDVI_{min}}{NDVI_{max} - NDVI_{min}} \times 100 \tag{2}$$

This empirical formula supplies a simple yet an effective way to estimate vegetation cover from remotely sensed data, frequently used in environmental monitoring and land cover assessments.

2.5. AHP modeling

The Analytic Hierarchy Process (AHP), first developed by Saaty [10], is a structured and powerful multi-criteria decision-making method widely employed to simplify complex problems by organizing them into hierarchical structures consisting of goals, criteria, and alternatives. By utilizing pairwise comparisons, AHP converts subjective assessments into objective numerical weights, facilitating systematic decision-making. Specifically, pairwise comparisons are quantified into a reciprocal matrix, and relative weights w_i are determined by calculating the principal eigenvector w from the matrix using the eigenvalue equation:

$$Aw = \lambda_{max} w \tag{3}$$

where A represents the pairwise comparison matrix, w denotes the eigenvector of priority weights, and λ_{max} indicates the largest eigenvalue of matrix A. This eigenvector method ensures consistency in the decision-maker's judgments [11]. Given its intuitive appeal and robust mathematical foundation, AHP has been extensively applied in various fields, including environmental planning, supply chain management, and urban development [12]. However, the validity of AHP results relies on minimizing inconsistencies in human judgment, which underscores the importance of rigorous consistency checks within the method.

2.6. Entropy modeling

Entropy modeling is a probabilistic approach commonly utilized in various fields, including information theory, data compression, and machine learning, to quantify the uncertainty or randomness within datasets or models [13]. At its core, entropy measures the amount of information or unpredictability contained in a random variable. The foundational concept of entropy was introduced by Claude Shannon, who defined entropy mathematically as:

$$H(X) = -\sum p(x_i) log_2 p\left(x_i\right) \tag{4}$$

where $p(x_i)$ represents the probability of occurrence of the event x_i[13]. In contemporary applications, entropy modeling has expanded significantly, guiding the development of efficient compression algorithms, neural network regularization techniques, anomaly detection in cybersecurity, and even ecological studies to assess biodiversity patterns [14]. Its versatility lies in its ability to quantify information effectively, making entropy modeling an indispensable analytical tool in numerous scientific and engineering disciplines.

3. Results and discussion

NDVI imagery offers critical insights into post-fire vegetation recovery, as demonstrated in the August Complex wildfire case. Analysis of data from 2020 to 2024 (Figure 1) reveals a marked decline in greenness (indicating dense vegetation) in 2021, followed by a gradual recovery from 2022 onward, with notable improvement by 2024. Spatial analysis further shows varied recovery rates across the region, likely influenced by localized factors such as soil moisture and fertility, while some areas remained sparsely vegetated, suggesting persistent issues like soil degradation.

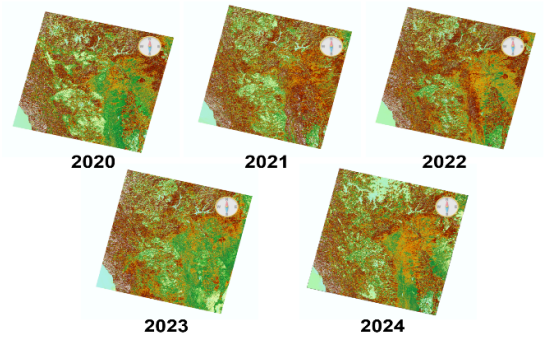

Figure 1. 2020-2024 NDVI images compilation for August Complex Wildfire

In summary, NDVI analysis highlights both the overall vegetation recovery post-wildfire and the variability of this recovery across different areas in petite detail. This shows the importance of custom ecological management and restoration that is adapted to fit local conditions.

Table 1. Calculation of AHP modeling parameter ratio

	Vegetation Coverage	Soil Recovery	Precipitation	Temperature	Wind	Ratio
Vegetation Coverage	1	2	3	3	3	0.39
Soil Recovery	1/2	1	2	2	2	0.23
Precipitation	1/3	1/2	1	3/2	5/6	0.13
Temperature	1/3	1/2	2/3	1	4/3	0.12
Wind	1/3	1/2	6/5	3/4	1	0.12

Table 2. Sum of AHP modeling score from 2020 to 2024

Parameter	Ratio	2020	2021	2022	2023	2024
Vegetation Coverage	0.39	7.6	1.4	4.2	5	6.6
Soil Recovery	0.23	7.4	1	3.6	4.6	6
Precipitation	0.13	4	3.6	5	7	6
Temperature	0.12	5.7	5.6	5.6	5.6	5.7
Wind	0.12	6	6.2	6.5	6.3	6.7
Sum	1	6.59	2.66	4.57	5.35	6.22

The environmental recovery following the August Complex Wildfire showed considerable variation from 2020 to 2024, with vegetation coverage and soil recovery playing the most critical roles according to the

weighted analysis conducted using the Analytic Hierarchy Process (AHP) (Table 1). Initially, in 2020, the environmental recovery index was robust (6.59), indicating favorable conditions that promoted strong vegetation regrowth and significant soil stabilization. However, a marked decline to 2.66 occurred in 2021, reflecting a severe setback specifically linked to the aftermath of the August Complex Wildfire, which significantly impaired vegetation and soil recovery processes during that year.

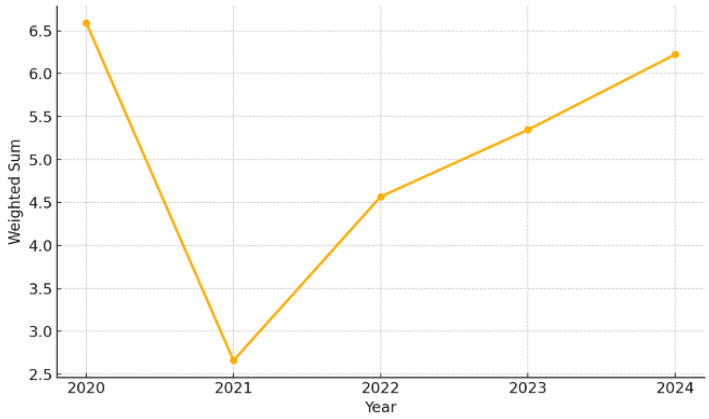

Figure 2. Sum of AHP modeling from 2020 to 2024

Following this initial decline, a steady improvement was observed from 2022 onwards, suggesting a resilient recovery dynamic (Figure 2). Vegetation coverage and soil recovery both improved gradually, supported by beneficial precipitation patterns, particularly noticeable in 2023 when rainfall notably increased. By 2024, the recovery index reached 6.22, closely approaching the initial recovery levels observed in 2020 (Table 2). These improvements highlight the importance of adequate rainfall in facilitating ecosystem recovery and underscore the resilience of vegetation and soil systems in bouncing back after setbacks caused by severe wildfire disturbances.

Temperature and wind exhibited limited influence on ecological recovery, remaining stable throughout the study period (Table 2). In contrast, vegetation and soil recovery emerged as the most critical factors, as identified by AHP analysis. The recovery index declined sharply from 6.59 in 2020 to 2.66 in 2021 due to wildfire impacts, but steadily improved thereafter, reaching 6.22 by 2024. This recovery was strongly supported by increased rainfall, particularly in 2023. Consequently, post-fire restoration strategies should prioritize plant regrowth and soil health in immediate post-fire years to enhance long-term ecological resilience.

Table 3. Score of entropy model from 2020 to 2024

Parameter	Ratio	2020	2021	2022	2023	2024
Vegetation Coverage	0.29	7.6	1.4	4.2	5	6.6
Soil Recovery	0.22	7.4	1	3.6	4.6	6
Precipitation	0.17	4	3.6	5	7	6
Temperature	0.16	5.7	5.6	5.6	5.6	5.7
Wind	0.16	6	6.2	6.5	6.3	6.7
Sum	1	6.384	3.126	4.796	5.556	6.238

The weighted sum analysis (Table 3) revealed a sharp decline from 6.384 in 2020 to 3.126 in 2021, reflecting severe environmental degradation caused by the historic August Complex wildfire. The fire considerably damaged vegetation, compromised soil stability, and negatively impacted overall ecosystem health. However, subsequent years showed a consistent recovery trend: scores improved to 4.796 in 2022, 5.556 in 2023, and reached 6.238 by 2024 (Figure 3), indicating gradual ecological regeneration likely aided by favorable climate conditions, natural regrowth, and restoration initiatives.

Despite this progress, the ecosystem had not fully returned to its pre-fire condition by 2024, underscoring the prolonged timeline required for complete recovery after major disturbances. These findings highlight the importance of sustained ecological monitoring and adaptive management strategies. Further research identifying key drivers of recovery—such as rainfall patterns, soil rehabilitation, or targeted revegetation—could enhance the effectiveness of future post-fire restoration efforts

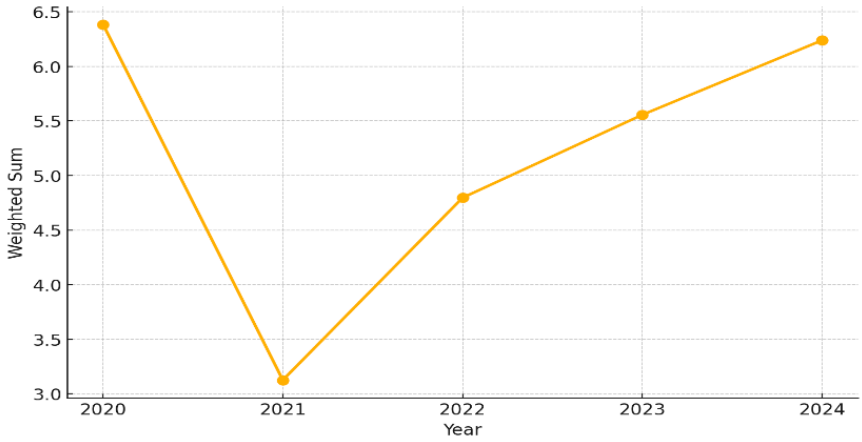

Figure 3. Sum of entropy modeling from 2020 to 2024

4. Conclusion

Events like the August Complex fire show just how badly wildfires can shake up everything from local wildlife to the air we breathe and the places people call home, but they also spotlight nature's tough bounce-back ability when we step in smartly. By leaning on tech like NDVI scans and layered decision models, we've gotten a clearer picture of the dragged-out recovery process, where stuff like plant regrowth and dirt quality really drive the comeback after these disasters. Looking bigger, this kind of work pushes for constant watchful eyes and flexible plans that fit the ground realities, helping cut down on threats ramped up by a warming world. In the end, getting a handle on these patterns doesn't just patch up scorched earth—it builds smarter ways to safeguard diverse life and keep communities safe in spots prone to flames everywhere.

Events comparable to the magnitude of the August Complex Fire show just how severe wildfires can truly be for their local ecosystems. Whether it's the local wildlife or the air quality in the aftermath, they can be completely turned upside down and take considerable amounts of time to recover. However, they also showcase the resiliency of nature when we intervene in a helpful way to accelerate recovery. By utilizing tech such as NDVI scans and layered decision models, we've been able to achieve a better understanding of nature's recovery process, helping us advance and develop more flexible recovery strategies. This kind of development allows for flexible plans that are suitable for real-world circumstances, helping to lessen threats in an increasingly warm world. In the end, gaining a better understanding of these patterns paves the way for us to better safeguard diverse life and to keep fire prone areas out of harm's way.

At the same time, the recovery process is deeply intertwined with human well-being, community stability, and questions of environmental justice. Differential recovery rates can influence which neighborhoods face prolonged risks—such as erosion, water insecurity, or degraded air quality—underscoring that ecological restoration is also a social and economic imperative. By connecting biophysical recovery patterns with the lived experiences of communities, this study highlights the importance of integrating scientific insights into policies that support resilience, equity, and long-term human–environment coexistence in fire-prone regions.

References

[1] Marlon, J. R., Bartlein, P. J., Gavin, D. G., Long, C. J., Anderson, R. S., Briles, C. E., ... Walsh, M. K. (2012). Long-term perspective on wildfires in the western USA. *Proceedings of the National Academy of Sciences, 109*(9), E535-E543.

[2] Chen, A., Tang, R., Mao, J., Yue, C., Li, X., Gao, M., ... Piao, S. (2020). Spatiotemporal dynamics of ecosystem fires and biomass burning-induced carbon emissions in China over the past two decades. *Geography and Sustainability, 1*(1), 47-58.

[3] Pereira, P., Bogunovic, I., Zhao, W., & Barcelo, D. (2021). Short-term effect of wildfires and prescribed fires on ecosystem services. *Current Opinion in Environmental Science & Health, 22*, 100266.

[4] Xing, Y. F., Xu, Y. H., Shi, M. H., & Lian, Y. X. (2016). The impact of PM2.5 on the human respiratory system. *Journal of Thoracic Disease, 8*(1), E69–E74. https://doi.org/10.3978/j.issn.2072-1439.2016.01.19

[5] O'Mara, T., Meador, A. S., Colavito, M., Waltz, A., & Barton, E. (2024). Navigating the Evolving Landscape of Wildfire Management: A Systematic Review of Decision Support Tools. *Trees, Forests and People, 100575*.

[6] Xiao, X., Hagen, S., & Zhang, Y. (2020). Post-fire recovery assessment using NDVI in the Amazon rainforest. *Remote Sensing of Environment, 242*, 111752.

[7] Pettorelli, N., Vik, J. O., Mysterud, A., Gaillard, J. M., Tucker, C. J., & Stenseth, N. C. (2005). Using the satellite-derived NDVI to assess ecological responses to environmental change. *Trends in Ecology & Evolution, 20*(9), 503–510.

[8] Carlson, T. N., & Ripley, D. A. (1997). On the relation between NDVI, fractional vegetation cover, and leaf area index. *Remote sensing of Environment, 62*(3), 241-252.

[9] Gutman, G., & Ignatov, A. (1998). The derivation of the green vegetation fraction from NOAA/AVHRR data for use in numerical weather prediction models. *International Journal of remote sensing, 19*(8), 1533-1543.

[10] Saaty, T. L. (1980). *The Analytic Hierarchy Process: Planning, Priority Setting, Resource Allocation*. McGraw-Hill, New York

[11] Saaty, T. L. (2008). Decision making with the analytic hierarchy process. *International Journal of Services Sciences, 1*(1), 83–98.

[12] Vaidya, O. S., & Kumar, S. (2006). Analytic hierarchy process: An overview of applications. *European Journal of Operational Research, 169*(1), 1–29.

[13] Shannon, C. E. (1948). A mathematical theory of communication. *The Bell system technical journal, 27*(3), 379-423. Chen, J., Wang, H., & Li, X. (2021). Application of AHP in post-fire ecosystem recovery assessment: A case study from Yunnan, China. *Environmental Science & Technology, 55*(4), 1234–1245.

[14] Jost, L. (2006). Entropy and diversity. *Oikos, 113*(2), 363-375.